Towards On-line Pose Measurement for Robots

Jan Böhm, Jürgen Hefele, Dieter Fritsch
email: first.last@ifp.uni-stuttgart.de

Institute for Photogrammetry
University of Stuttgart
Geschwister-Scholl-Str. 24, 70174 Stuttgart, Germany

Abstract. We present a photogrammetric system for on-line pose measurement of a robot. The system is based on photogrammetric measurement techniques, namely resection. We describe the theoretical foundations of our approach as well as early details of our implementation and hardware set-up. The results achieved are compared to those of a commercial ball-bar system.

1 Introduction

While industrial robots typically can achieve a repeatability of 0.1 mm or less, their absolute accuracy can be in the range of only 1 mm or worse. Many new applications in robotics, including flexible optical measurement, require improved absolute accuracy. Photogrammetry has been used for several years to perform off-line calibration in order to increase accuracy. However when operating a robot under shop-floor conditions the accuracy is expected to decrease again over time. Clearly an on-line pose correction is desirable. We present a system for the on-line pose measurement based on photogrammetry.

2 Photogrammetric System

Photogrammetric measurement is based on the classical collinearity equations defining the condition, that the projection center, a point in object space and its corresponding point on the image plane are on a straight line. Let c be the principal distance of the camera, (X_0, Y_0, Z_0) the principal point, (X, Y, Z) the coordinates of the object point and (x, y) the coordinates of the corresponding image point. Then the collinearity equation is (see [7])

$$\begin{aligned} x &= x_0 - c\frac{(X-X_c)r_{11}+(Y-Y_c)r_{12}+(Z-Z_c)r_{13}}{(X-X_c)r_{31}+(Y-Y_c)r_{32}+(Z-Z_c)r_{33}} = x_0 - c\frac{Z_x}{N} \\ y &= y_0 - c\frac{(X-X_c)r_{21}+(Y-Y_c)r_{22}+(Z-Z_c)r_{23}}{(X-X_c)r_{31}+(Y-Y_c)r_{32}+(Z-Z_c)r_{33}} = y_0 - c\frac{Z_y}{N} \end{aligned}$$

with the condition that r_{ij} are the elements of a 3-D orthogonal rotation matrix. For many applications in photogrammetry the rotation matrix R is parameterized using Cardan angles ω, ϕ, κ. However, it has shown to be favorable

(see [10]) to use a parameterization using quaternions. We use Hamilton normalized quaternions to describe a rotation matrix:

$$R = (I+S)(I-S)^{-1},\ S = \begin{bmatrix} 0 & -c & b \\ c & 0 & -a \\ -b & a & 0 \end{bmatrix}$$

2.1 Camera Model

While the basic camera model in photogrammetry is the pin-hole camera, additional parameters are used for a more complete description of the imaging device. The following parameters are based on the physical model of D. C. Brown ([1]). We follow the notation for digital cameras presented by C. S. Fraser ([3]). Three parameters K_1, K_2 and K_3 are used to describe the radial distortion. Two parameters P_1 and P_2 describe the decentring distortions. Two parameters b_1 and b_2 describe a difference in scale between the x- and y-axis of the sensor and shearing. To obtain the corrected image coordinates (x, y) the parameters are applied to the distorted image coordinates (x', y') as follows

$$\begin{aligned}
\overline{x} &= x' - x_0 \\
\overline{y} &= y' - y_0 \\
\triangle x &= \overline{x}r^2K_1 + \overline{x}r^4K_2 + \overline{x}r^6K_3 + (2\overline{x}^2 + r^2)P_1 + 2P_2\overline{xy} + b_1\overline{x} + b_2\overline{y} \\
\triangle y &= \overline{y}r^2K_1 + \overline{y}r^4K_2 + \overline{y}r^6K_3 + 2P_1\overline{xy} + (2\overline{y}^2 + r^2)P_2 \\
x &= \overline{x} + \triangle x \\
y &= \overline{y} + \triangle y
\end{aligned}$$

Where (x_0, y_0) is the principal point and $r = \sqrt{\overline{x}^2 + \overline{y}^2}$ is the radial distance from the principal point. The camera's parameters are determined in a bundle adjustment using a planar test field. The bundle adjustment process is carried out before-hand.

2.2 Resection

The problem of (spatial) resection involves the determination of the six parameters of the exterior orientation of a camera station. We use a two-stage process to solve the resection problem. A closed-form solution using four points gives the initial values for an iterative refinement using all control points.

Closed-form Resection Several alternatives for a closed form solution to the resection problem were given in literature. We follow the approach suggested by Fischler et. al. [2]. Named the "Perspective 4 Point Problem" their algorithm solves for the three unknown coordinates of the projection center when the coordinates of four control points lying in a common plane are given. Because the control points are all located on a common plane the mapping in-between image- and object points is a simple plane-to-plane transformation T. The location of

the projection center can be extracted from this transformation T when the principal distance of the camera is known. For a detailed description of the formulas please refer to the original publication.

To complete the solution of the resection problem we also need the orientation of the camera in addition to its location. Kraus [8] gives the solution for determining the orientation angles when the coordinates of the projection center are already known. The algorithm makes use of only three of the four points.

Iterative Refinement The closed-form solution makes use of only four control points. Usually much more control points are available and the solution is more accurate if all observations are used in a least squares adjustment. For an iterative solution, the collinearity equations have to be linearized. This is standard in photogrammetry. While most of the partial derivatives of the classical bundle adjustment remain the same, the elements for rotation have changed because of our use of quaternions . Six new partial derivatives replace the common $\frac{\partial \xi}{\partial \omega}, \frac{\partial \xi}{\partial \phi}, \ldots$:

$$\begin{aligned}
\frac{\partial \xi}{\partial b} &= \frac{-2f}{N^2 D}(-Z_x^2 + cZ_xZ_y - aZ_yN - N^2) \\
\frac{\partial \xi}{\partial a} &= \frac{-2f}{N^2 D}(cZ_x^2 + Z_xZ_y + bZ_yN + cN^2) \\
\frac{\partial \xi}{\partial c} &= \frac{-2f}{N^2 D}(-aZ_x^2 - bZ_xZy + Z_yN - aN^2) \\
\frac{\partial \eta}{\partial b} &= \frac{-2f}{N^2 D}(-Z_xZ_y + aZ_xN + cZ_y^2 + cN^2) \\
\frac{\partial \eta}{\partial a} &= \frac{-2f}{N^2 D}(cZ_xZ_y - bZ_xN + Z_y^2 + N^2) \\
\frac{\partial \eta}{\partial c} &= \frac{-2f}{N^2 D}(-aZ_xZ_y - Z_xN - bZ_y^2 - bN^2)
\end{aligned}$$

Using the results from the closed-form solution as described above, we can now iteratively refine the solution for all control points available.

Simulated Results Simply using the formulas given above and applying error propagation we can now do a simulation of the resection to predict the expected errors in resection. Assuming a focal length of $12\,mm$ and with a standard pixel size of $6.7\,\mu m$, the expected errors in x, y and z for a certain error in image measurement are given in table 1.

3 Implementation

The algorithms described above were implemented in an on-line pose measurement system. The systems components, both mechanical and electronic are described below. In addition the test configuration using an industrial robot is described.

3.1 Hardware

The optical sensor we are using is a Basler A113 camera, with a Sony CCD chip, which has a resolution of 1300×1030 pixels. The camera provides a digital

output according to IEEE standard RS644. A frame-grabber is integrated into a standard PC. The digital camera system is superior to an analog camera system since it does not exhibit line jitter problems thus enabling more precise measurements. Schneider-Kreuznach lenses with $12mm$ focal length are mounted onto the camera.

To maximize the signal intensity we use retro-reflective targets and a ring light on the camera. To minimize the effects of external light sources we use near-infrared LEDs as light source and a filter on the lens. (see figure 1, left)

The control points are fixed onto a plane, also used as a calibration plate. We use coded targets to achieve automated identification of the targets. The circular center of the target is used for sub-pixel precise measurement of the targets position. A circular code surrounding the center carries a binary representation of the unique identifier. (see figure 1, center)

The set-up for our experiments consists of a Kuka KR15 robot. It is a six axis robot with a maximum payload of 15 kg at maximum range of 1570 mm. The robot is specified with a repeatability of ± 0.1 mm. The absolute accuracy is not specified.

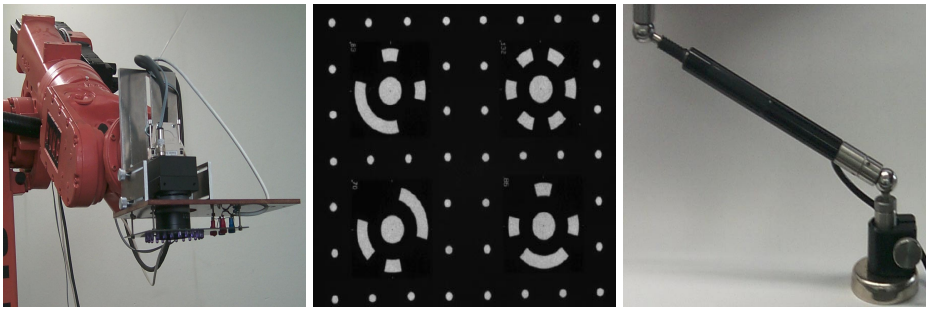

Fig. 1. Left: camera and ring LED mounted onto the robot. Center: part of the test field. Right: Ball-bar tester.

3.2 Image Processing

Image processing is performed on a standard PC. The images are first binarized using an optimal thresholding algorithm introduced by Otsu (see [9]). Then a consistent component labeling is performed to find targets. We discriminate the circular centers from all other 'blobs' by size and a simple shape-test. Since the targets can be smaller than 10 pixels in diameter we do not perform ellipse fitting (see [4]). The center of the target is computed as the weighted centroid.

In addition the elliptic axes and the pose angle are computed. The center, the axes and the angle are used to determine the code ring. The code ring is read with six-times oversampling. The acyclic redundant code provides unique identifiers for up to 352 targets.

In addition to the coded target much smaller uncoded targets were added to the test field. After the closed-form resection has been computed using the coded targets, the approximate position of these targets can be projected onto the image since their three-dimensional location is known from calibration. Thus these additional targets can be easily identified through their position.

3.3 Results

The sensor delivers a frame rate of about 12 frames per second. The implemented system is capable to process a single image in $420ms$. A typical image will contain about 30 coded and about 200 uncoded targets. This gives us a processing speed of 500 targets per second including all image processing steps and the resection. The standard deviations obtained in a first test run are given in table 1.

standard deviations	simulation		test-run
image measurement	$\frac{1}{5}$pixel	$\frac{1}{10}$pixel	...
resection in x	0.06 mm	0.03 mm	0.2 mm
resection in y	0.06 mm	0.03 mm	0.2 mm
resection in z	0.02 mm	0.009 mm	0.06 mm

Table 1. Standard deviations of resection.

4 Circular Test

ISO 230-4 [6] describes the "Circular tests for numerically controlled machine tools". While these test were originally designed for the simultaneous movement of only two axes, they also have valid implications for other machines. When the test is carried out the robot performs a circular motion and a measurement system detects any deviation from the ideal path. The parameters of the test include

1. diameter of the nominal path
2. contouring feed
3. machine axes moved to produce the actual path

The results of the test include the radial deviation F, which is defined as the deviation between the actual path and the nominal path, where the center of the nominal path can be determined either by manual alignment or by least squares adjustment.

4.1 Ball-bar System

There exist several commercial systems to perform the circular test. We chose as a reference system the Renishaw ball-bar system. The system consists mainly

of a linear displacement sensor which is placed between two ball-mounts, one near the tool center point (TCP) of the machine and one in the center of the circular path. The displacement sensor continually measures the distance of the two balls and thereby measures any deviations in the radius of the circular path. (see figure 1, right)

The device has a length of 150 mm, a measurement resolution of 0.1 μm, an approximate accuracy of 1 μm and a measurement range of ± 1 mm. It is able to measure the deviation at a frequency of 300 Hz.

For the actual test we programmed a circular path of 149.9 mm to ensure the system will stay within its measurement range. The contouring feed was 10 mm/s. Because the TCP orientation was programmed to be constant, all six axes of the robot were moved to produce the path.

4.2 Photogrammetric Test

For the test of our own system we used exactly the same circular path of the robot. The calibration plate was placed on the floor, the camera looking down onto it. The circular path, the calibration plate and the image plane were all approximately parallel to each other. Our online system continuously records the six parameters of the exterior orientation. The projection center coordinates are used to compute the least squares adjustment of the circular path to determine the center and radius of the ideal path, as suggested by ISO 230-4. The deviation of the measured coordinates of the projection center to the ideal path is the radial deviation. The deviations in the rotation angle is also recorded. This feature is not available in the ball-bar test.

4.3 Results

Figure 2 shows the results of the circular test. We see that currently we are unable to achieve the same accuracies as the commercial ball-bar system. The deviations in rotation mentioned above are significant since the camera is mounted onto the robot with a certain distance ($\sim$ 100 mm) from the TCP. Therefore the deviations in the projection center not only represent deviations in the position of the TCP but also in its rotation. We can clearly see from figure 2(c) how extreme deviations in orientation correspond to extreme deviations in position. Since the ball-mount of the ball-bar tester is located much closer ($\sim$ 10 mm) to the true TCP, it is less sensitive to errors in rotation.

5 Summary

The implemented system is an improvement of our off-line system published earlier [5]. It has proven to be quite flexible and we believe it can be easily integrated into many application in robotics, especially applications in optical measurement. Currently the accuracies do not compare well to those of a commercial ball-bar system. However the deviations are mostly due to an error in

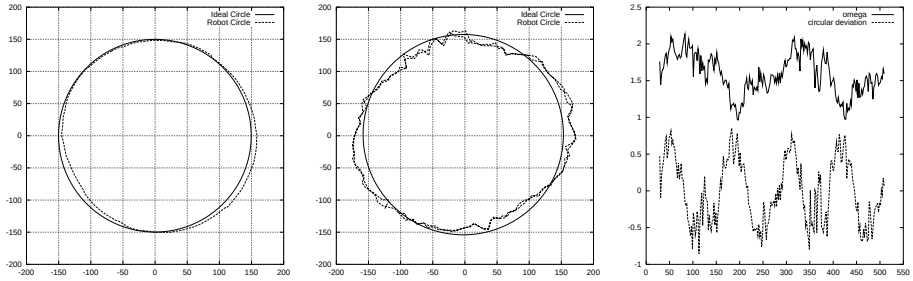

(a) (b) (c)

Fig. 2. Results of the circular test (a) for the ball-bar system the movement of the ball-mount center is shown)and (b) for the photogrammetric system the movement of the camera's projection center is shown in mm. Deviations are magnified by a factor of 25. (c) Angular deviation and radial deviation.

the robots TCP orientation. For future work the deviations measured at the projection center should be re-transformed to the TCP from the known hand-eye calibration matrix. To achieve on-line pose correction the obtained pose information has to be passed directly to the robot control unit.

References

1. Duane C. Brown. Close-range camera calibration. *Photogrammetric Engineering*, 37(8):855–866, 1971.
2. M. A. Fischler and R. C. Bolles. Random sample consensus: A paradigm for model fitting with applications to image analysis and automated cartography. *Communications of the ACM*, 24(6):381–393, June 1981.
3. Clive S. Fraser. Digital camera self-calibration. *ISPRS Journal of Photogrammetry and Remote Sensing*, 52:149–159, 1997.
4. Clive S. Fraser and Juliang Shao. An image mensuration strategy for automated vision metrology. In A. Gruen and H. Kahmen, editors, *OPtical 3-D Measurement techniques IV*, pages 187–197. Wichmann, September 1997.
5. Juergen Hefele and Claus Brenner. Robot pose correction using photogrammetric tracking. In *Machine Visiobn and Three-Dimensional Imagin Systems for Inspection and Metrology*. SPIE, SP, November 2000.
6. ISO. *Test code for machine tools - Part 4: Circular tests for numerically controlled machine tools*, August 1996.
7. K. Kraus. *Photogrammetrie Band 1.* Dümmler, 1984.
8. K. Kraus. *Photogrammetrie Band 2.* Dümmler, 1996.
9. N. Otsu. A threshold selection method from grey-level histograms. *SMC*, 9:62–66, January 1979.
10. Senlin Zhang. Anwendungen der drehmatrix in hamilton normierten quaternionen bei der bündelblockausgleichung. *ZfV*, 4:203–210, 1994.